Cation ordering in Ni–Fe olivines

HANS ANNERSTEN, TORE ERICSSON AND ANESTIS FILIPPIDIS

Department of Mineralogy and Petrology
Institute of Geology, University of Uppsala
Box 555, S-751 22 Uppsala, Sweden

Abstract

Synthetic nickel–iron olivines, equilibrated at 1000°C, were investigated by means of Mössbauer spectroscopy at high and low temperature. A strong tendency towards an ordering of Ni^{2+} into the M1 site and Fe^{2+} into M2 was observed. K_D for the exchange reaction $Ni^{2+}(M1) + Fe^{2+}(M2) \rightleftarrows Fe^{2+}(M1) + Ni^{2+}(M2)$ varies little with chemical composition, suggesting a near ideal solid solution in Ni–Fe olivines. Gibbs free energy of exchange at 1000°C is calculated to be 6.0 kcal/mole (24.9 kJ/mole).

Introduction

Nickel is an important constituent which usually fractionates into olivine in early magmatic crystallization (Wager and Mitchell, 1951). Olivines containing nickel are usually found in ultramafic rocks of possible upper-mantle origin. The most nickel-rich olivine, liebenbergite, with composition $(Ni_{1.52}Mg_{0.33}Co_{0.05}Fe_{0.12})SiO_4$, has been described by de Waal and Calk (1973). Nickel-bearing olivine is usually Mg-dominant, although a complete solid solution of Ni_2SiO_4 and Mg_2SiO_4 was observed by Akomoto *et al.* (1976). In most natural olivines, however, iron is the second most important solid solution constituent. This paper reports on an investigation of the Ni_2SiO_4–Fe_2SiO_4 solid solution.

The potential use of intracrystalline order–disorder among the non-equivalent M1 and M2 sites in olivines for estimating rock-forming temperature provides incentive for studying the distribution within this mineral (see *e.g.,* Brown, 1980). The intracrystalline Fe–Mg distribution in olivines is still in debate and has been observed to be temperature dependent by Virgo and Hafner (1972) and Finger and Virgo (1971), or dependent on oxygen fugacity as suggested by Will and Nover (1979). A third possibility is the influence of a third element, for example Ni.

Studies of solid solutions of transition elements such as Ni (Rajamani *et al.,* 1975; Wood, 1974; Bish, 1981), Co (Ghose and Wan, 1974), and Zn (Brown, 1970) in forsterite have shown an enrichment of these elements into the M1 site, whereas Mn (Francis and Ribbie, 1980) fractionates into the

M2 sites in olivines. The observed cation ordering is explained in part by the crystal field stabilization energy criteria (CFSE) or, for ions yielding zero CFSE (Mn,Zn), by ionic size criteria or covalency effects. In the present study, Ni^{2+} and Fe^{2+} are both affected by the crystal field, predicting a less ordered distribution in Ni–Fe olivines than in Ni–Mg olivines. On the other hand, according to the ionic size criteria, the difference in the ionic radii ($Fe^{2+} = 0.77$, $Ni^{2+} = 0.70$Å) suggests an ordering of Ni^{2+} into the smaller M1 site. the observed fractionation of certain transition metal ions, usually observed in minor amounts in natural olivines, may be partly responsible for the observed variations in element distribution in natural Fe–Mg olivines.

Synthesis and experimental results

Synthetic olivines were produced from oxide mixtures (*p.a.* grade SiO_2, Fe_2O_3, metallic Fe and NiO). Crystallization of olivines was performed with the mixtures in gold capsules in an internally heated autoclave for 140 hours at 1000°C (pressure: 1.0 ± 0.1 kbar) using argon as pressure medium. Samples H 11 and H 12 were crystallized from melts held at ~2000°C in an arc furnace in an argon atmosphere, and were afterwards annealed at 1000°C for 168 hours in evacuated silica tubes ($<10^{-3}$ torr) and quenched to room temperature.

Optical examination of the products showed the presence of trace amounts of opaque phases (magnetite, Ni–Fe alloy) and of quartz in some runs. The opaque phases were carefully removed under acetone by use of a hand magnet. X-ray diffraction

analysis and Mössbauer spectroscopy studies later show no sign of impurities remaining in the samples. Cell parameter refinements (Table 1 and Fig. 1) on the synthetic olivines were performed with X-ray powder diffraction data (13 to 26 reflections) using a computer program (CELNE) assuming space group *Pbnm*. The crystal size obtained from the synthetic runs was large enough (~10 μm) to allow microprobe analysis of at least three grains from each run. Values given in Table 1 are average values, obtained from computer corrected data. Within the limit of the analyzing technique no significant zoning or inhomogeneity of the olivine grains was observed.

Mössbauer spectra of powder samples were obtained with the absorber held at an elevated or low temperature. This increases the resolution of the absorption pattern arising from ^{57}Fe in M1 and M2 sites (Bush *et al.*, 1970; Kündig *et al.*, 1967). The temperature was regulated within ±1°. Spectra were accumulated in a multichannel analyzer (512 channels) operating in multi-scaling mode. The electro-mechanical vibrator was driven with a constant magnitude of acceleration and the mirror symmetric spectra were folded and summed before the computer analysis (Agresti *et al.*, 1969). Co in Rh was used as a source, always at room temperature, and centroid shifts are given relative to metallic Fe. Mössbauer results are shown in Table 2.

The occupation of Fe at the M1 and M2 sites is obtained from the area ratios (Table 3) of the computer fitted Mössbauer spectra (Figs. 2 and 3).

Table 1. Composition and cell parameters of synthetic olivines

|	17	H 14	15	16	H 11	H 12
SiO$_2$ wt-%	29.5	28.8	29.7	29.3	28.2	28.3
FeO	71.8	63.5	61.1	58.2	34.9	17.4
NiO	0.0	6.5	8.5	12.6	33.9	53.8
Σ	101.3	98.8	99.3	100.1	97.0	99.5
Number of ions on the basis of 4 oxygens						
Si	0.99	0.99	1.01	1.00	1.00	0.99
Fe^{2+}	2.02	1.83	1.74	1.66	1.03	0.51
Ni	0.00	0.18	0.23	0.35	0.97	1.51
x^{Fe}	1.00	0.91	0.88	0.83	0.52	0.25
x^{Ni}	0.00	0.09	0.12	0.17	0.48	0.75
Cell parameters (space group Pbnm)						
a Å	4.821(1)	4.807(1)	4.797(1)	4.788(1)	4.779(6)	4.738(1)
b	10.478(2)	10.457(2)	10.447(3)	10.437(2)	10.335(5)	10.241(2)
c	6.092(2)	6.078(2)	6.075(2)	6.066(1)	6.019(5)	5.976(1)
V Å^3	307.7	305.5	304.4	303.1	297.3	290.0
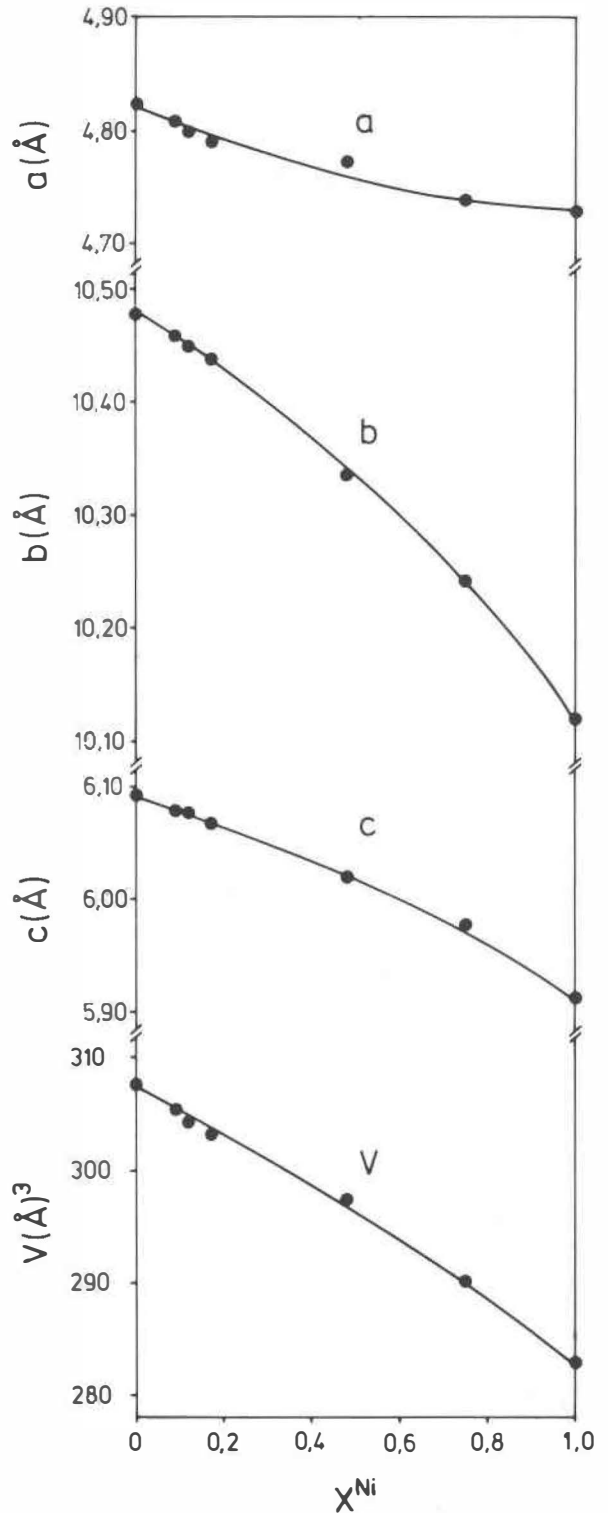
Fig. 1. Cell parameter variations with composition of synthetic Ni–Fe-olivines. Values for Ni$_2$SiO$_4$ from Brown (1970).

Table 2. Mössbauer parameters of ^{57}Fe in synthetic olivines

Sample	T,K	H_{eff} M1	M2	IS M1	M2	ΔE_Q M1	M2	Width
17	6	31.8	12.1	1.29	1.32	3.27	3.05	0.38
17	540	0	0	0.91	0.98	1.99	2.47	0.24
17	673	0	0	0.83	0.90	1.76	2.25	0.24
H 14	673	0	0	0.83	0.90	1.78	2.26	0.24
15	673	0	0	0.83	0.89	1.78	2.25	0.26
16	6	nd	12.3	nd	1.33	nd	3.13	0.35
16	680	0	0	0.82	0.89	1.77	2.22	0.25
H 11	9	nd	12.3	nd	1.33	nd	3.10	0.38
H 11	673	0	0	0.83^x	0.91	1.98	2.28	0.32
H 12	6	-	12.1	-	1.34	-	3.09	0.50
H 12	820	-	0	-	0.79	-	1.95	0.29

H_{eff} given in Tesla. IS, ΔE_Q and Width given in mm/s (±0.01).
IS given relative to metallic iron at room temperature.
^{x} constrained

Assignments of the ^{57}Fe resonance pattern are made in agreement with Warburton (1978), Kündig et al. (1967), Karyagin (1966), and van Dongen Tornman et al. (1975). High-temperature spectra have been corrected for different recoil-free fractions of iron in the M1 and M2 sites. The M1 pattern in the low-temperature spectra is considerably broadened with increasing Ni-content, making precise determination of the Mössbauer parameters very difficult. However, as seen from Figure 3, the M1 pattern is completely lacking in the most iron-poor sample H 12.

Table 3. Site occupancy in synthetic olivines

Sample	T,K	X_{01}^{Fe}	Area % M1	M2	X^{Fe} M1	M2	K_D
17	6	1.00	49.2	50.8			
17	560	1.00	49.5	50.5			
17	673	1.00	48.6	51.4	1.00	1.00	
H 14	673	0.91	45.4	54.6	0.87	0.99	0.07(3)
15	673	0.88	43.2	56.8	0.77	0.96	0.14(3)
16	6	0.83	~30	~70			
16	680	0.83	40.4	59.6	0.69	0.96	0.09(3)
H 11	9	0.52	~10	~90			
H 11	673	0.52	23.1	76.9	0.24	0.80	0.08(4)
H 12	6	0.25	~0	~100	~0	0.25	~0.00
H 12	820	0.25	~0	~100	~0	0.25	~0.00

$$K_D = \frac{X_{M1}^{Fe} \cdot (1 - X_{M2}^{Fe})}{X_{M2}^{Fe} \cdot (1 - X_{M1}^{Fe})}$$
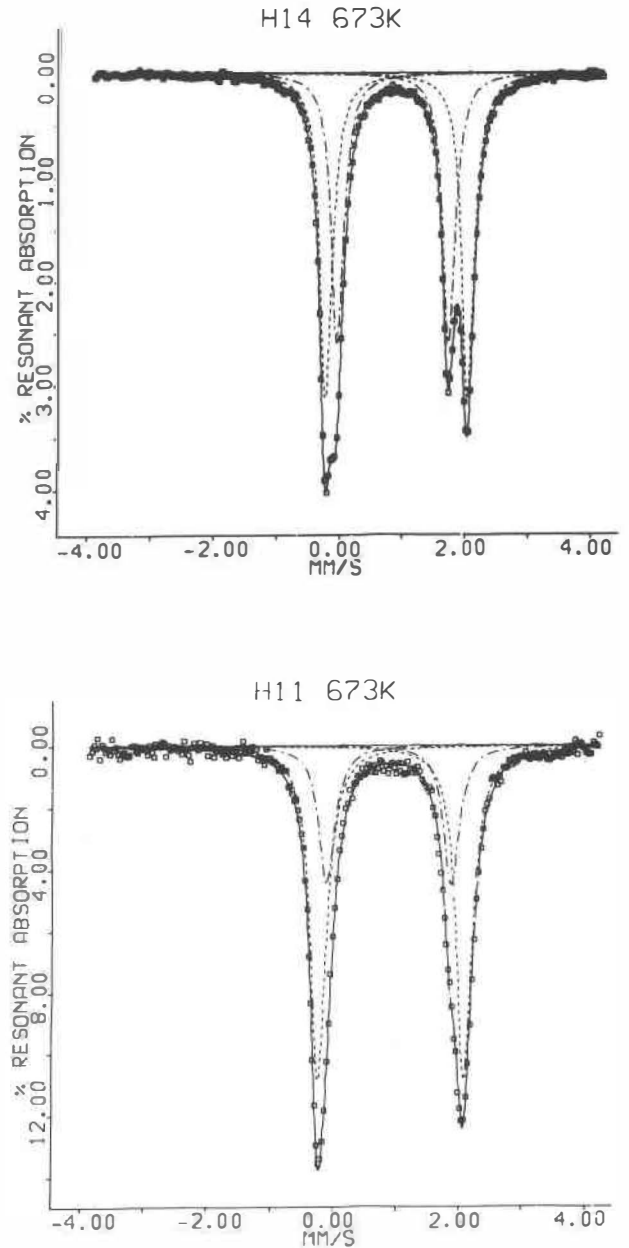

H14 673K

H11 673K

Fig. 2. Mössbauer spectra of samples H 14 and H 11 at 673 K. ⋯ M1 site, --- M2 site.

Discussion

Ni–Fe distribution in olivine

The almost linear decrease in volume with increasing Ni-content in fayalite indicates a small deviation from Vegard's law. The slight increase in the slope of the volume change beyond $X^{Ni} = 0.5$ may suggest an increasing substitution of the small Ni^{2+} ion into the larger M2 site in olivine. This is

further supported by the distribution coefficients (K_D) obtained from the Mössbauer spectra (*cf.* Table 3). K_D for ionic distribution of Fe^{2+} and Ni^{2+} between the two non-equivalent sites is defined by:

$$K_D = \frac{X_{M1}^{Fe} (1 - X_{M2}^{Fe})}{X_{M2}^{Fe} (1 - X_{M1}^{Fe})}$$

The observed K_D-values indicate a strong preference for Ni^{2+} to enter the M1 site in competition with Fe^{2+} in olivine.

The intracrystalline exchange in Ni–Fe olivine may be expressed by the following reaction

$$Ni^{2+}(M1) + Fe^{2+}(M2) \rightleftarrows Ni^{2+}(M2) + Fe^{2+}(M1)$$

with the following equilibrium constant:

$$K_a = \frac{a_{M1}^{Fe} \cdot a_{M2}^{Ni}}{a_{M2}^{Fe} \cdot a_{M1}^{Ni}}$$

The small variation in the observed values of K_D (*cf.* Table 3) for different compositions in olivine may indicate that the activity coefficient approaches unity and the solid solution of Fe^{2+} and Ni^{2+} in
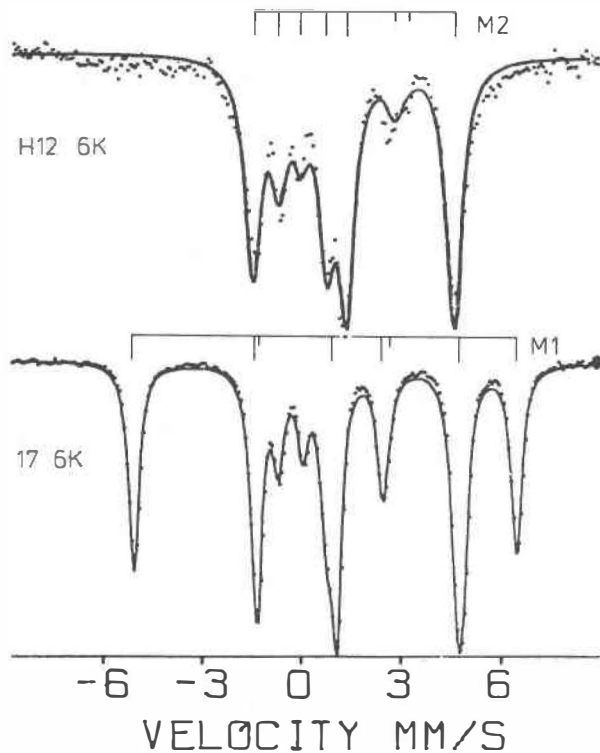

Fig. 3. Mössbauer spectrum of magnetically ordered olivine at 6 K. Upper spectrum sample H 12 with iron apparently only in M2. Lower spectrum sample 17 with both M1 and M2 equally populated by iron. Forbidden transitions shown by small bars.

olivine is close to ideal, in agreement with earlier observations at elevated temperature (Saxena, 1973). K_D can therefore be set equal to K_a and the Gibbs free energy change $\Delta G° = -RT\ln K_D$, can be estimated from the observed distribution values. The calculated average value at 1000°C is 6.0 kcal/mole (24.9 kJ/mole). The observed high degree of ordering of the ions in Ni–Fe olivines is in good agreement with the prediction from ionic size criteria. They are markedly more ordered than Ni–Mg olivines as expected from the smaller difference between Mg^{2+} and Ni^{2+} ionic radii (Rajamani *et al.*, 1975). The strong influence on the distribution from ionic size differences is further supported by the observed intracrystalline distribution in Mn–Fe olivines, where the larger Mn^{2+} ion strongly fractionates into M2 in competition with the smaller Fe^{2+} ion (*cf.* Fig. 4).

Crystal field stability theory also predicts a strong ordering of Ni^{2+} into the M1 site (Burns, 1970). Indeed Walsh *et al.* (1974) suggested that Fe^{2+} gains extra CFSE at M2 by the dynamic Jahn–Teller effect from the trigonal distortion of the M2 site in olivine. This feature would then explain the increased ordering in Ni–Fe olivines relative to Ni–Mg olivines observed for synthetic olivines (Rajamani *et al.*, 1975; Bish, 1981). Bish (1981) also investigated a natural Ni–Fe–Mg-bearing olivine ($Ni_{1.52}Co_{0.05}Fe_{0.09}Mg_{0.32}$)$SiO_4$ approaching our sample H 12 in composition. The natural sample (estimated equilibration temperature 730°C) was found to be fully ordered with the M1 site exclusively populated by Ni^{2+}. Our sample H 12, annealed at 1000°C, indicates a similar ordering.

Bonding of iron

Some quantitative data regarding the bonding of iron in Ni–Fe olivine are obtained from the Mössbauer parameters given in Table 2. Quadrupole splittings, sensitive to the near surroundings of the iron nucleus, generally increase with increasing nickel-content of the solid solutions, and are markedly more at the M1 site. This is in agreement with the expected smaller distortion of the M1 site with increasing occupancy by the smaller Ni^{2+} ion (Brown, 1980). At low temperature (6 K), however, the M1 site shows a larger splitting compared to the less distorted M2 site. The observed quadrupole splitting is a combined effect of the crystalline field, spin-orbit interaction and core polarization. The latter features are expected to change at low temperature close to absolute zero, thereby resulting in
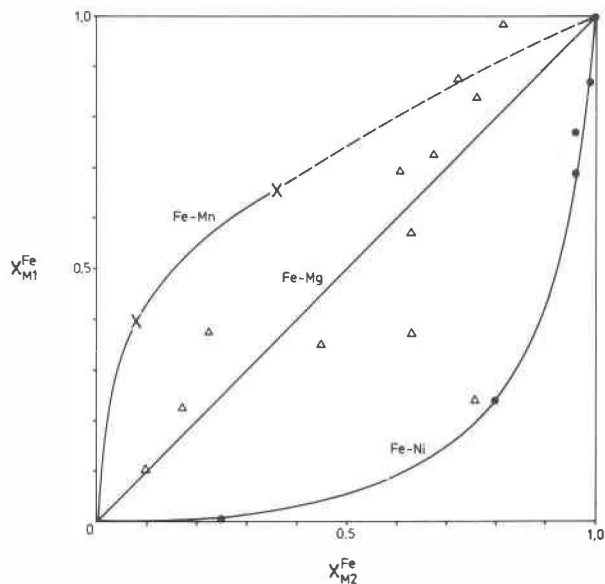
Fig. 4. Iron distribution in olivines. ● Fe–Ni-olivines (this study), △ Fe–Mg-olivines (Warburton, 1978), X Fe–Mn-olivines (Brown, 1970).

an increased quadrupole splitting. This effect should be markedly larger at a distorted site.

Isomer shifts are consistently smaller for iron in the M1 site. It can be expected that a decrease in the volume of the coordination polyhedron would lead to an increased electron density and hence, in the case of ^{57}Fe, a decrease in the value of the isomer shift (Tang Kai *et al.*, 1980).

Conclusions

Nickel orders highly preferentially into the M1 site in fayalite: the ordering is more pronounced than in forsterite of similar nickel-content. The difference in effective ionic radius between Fe^{2+} and Ni^{2+} is expected to be the dominant reason for the observed fractionation between M1 and M2 sites in olivine. Both ions are stabilized by the crystal field, however, and the observed ordering is in agreement with the observed crystal field stabilization energies for Ni^{2+} and Fe^{2+} in olivines. Evidence from the X-ray data and the observed compositional variation of the distribution coefficient (K_D) shows that the solid solution in Ni–Fe olivine is close to ideal at 1000°C.

References

Agresti, D., Bent, M., and Persson, B. (1969) A versatile computer program for analysis of Mössbauer Spectra. Nuclear Instrument Methods, 72, 235–236.

Akimoto, S., Matsui, Y., and Syono, Y. (1976) High pressure crystal chemistry of orthosilicates and the formation of the mantle transition zone. In J.-G. Strens, Ed., The Physics and Chemistry of Minerals and Rocks, p. 327–363. John Wiley & Sons, New York.

Bish, D. L. (1981) Cation ordering in synthetic and natural Ni–Mg olivines. American Mineralogist, 66, 770–776.

Brown, G. E. (1970) The Crystal Chemistry of Olivines. Ph.D. Thesis, Virginia Polytechnic Institute and State University, Blacksburg, Virginia.

Brown, G. E. (1980) Olivines and silicate spinels. In P. H. Ribbe, Ed., Orthosilicates, Reviews in Mineralogy, p. 275–281. Mineralogical Society of America, Washington, D. C.

Burns, R. G. (1970) Mineralogical Applications of Crystal Field Theory. Cambridge University Press, Cambridge.

Bush, W. R., Hafner, S. S. and Virgo, D. (1970) Some ordering of iron and magnesium at the octahedral coordinated sites in a magnesium-rich olivine. Nature, 227, 1339–1341.

van Dongen Torman, J., Jogannathan, R. and Trooster, J. M. (1975) Analysis of ^{57}Fe Mössbauer hyperfine spectra. Hyperfine Interactions, 1, 135–144.

Finger, L. W. and Virgo, D. (1971) Confirmation of Fe/Mg ordering in olivine. Carnegie Institute of Washington Year Book, 70, 221–225.

Francis, C. A. and Ribbe, P. H. (1980) The forsterite–tephroite series: Crystal structure refinements. American Mineralogist, 65, 1259–1263.

Ghose, S. and Wan, C. (1974) Strong site preference of Co^{2+} in olivine $Co_{1.10}Mg_{0.90}SiO_4$. Contributions to Mineralogy and Petrology, 47, 131–140.

Karyagin, S. W. (1966) Determination of the local field parameters in Mössbauer hyperfine spectra. Soviet Physics-Solid State, 8, 391–396.

Kündig, W., Cape, J. A., Lindqvist, R. H. and Constararis, G. (1967) Some magnetic properties of Fe_2SiO_4 from 4 K to 300 K. Journal of Applied Physics, 38, 947–948.

Rajamani, V., Brown, G. E. and Prewitt, C. T. (1975) Cation ordering in Ni–Mg olivine. American Mineralogist, 60, 292–299.

Saxena, S. K. (1973) Thermodynamics of Rockforming Crystalline Solid Solutions. Springer Verlag, New York.

Tang Kai, A., Annersten, H. and Ericsson, T. (1980) Molecular orbital (MSXα) calculations of s-electron densities of tetrahedrally coordinated ferric iron: comparison with experimental isomer shifts. Physics and Chemistry of Minerals, 5, 343–349.

de Waal, S. A. and Calk, L. (1973) Nickel minerals from Baberton, South Africa: VI. Liebenbergite, a nickel olivine. American Mineralogist, 58, 733–735.

Wager, L. R. and Mitchell, R. L. (1951) The distribution of trace elements during strong fractionation of basic magma. Geochimica et Cosmochimica Acta, 1, 129–208.

Walsh, D., Donnay, G. and Donnay, J. D. H. (1974) Jahn–Teller effects in ferro-magnesian minerals: pyroxenes and olivines. Bulletin de la Société française de Minéralogie et de Cristallographie, 97, 170–183.

Warburton, D. L. (1978) Mössbauer effect studies of olivines. Ph.D. Thesis, The University of Chicago, Chicago, Ill.

Will, G. and Nover, G. (1979) Influence of oxygen partial pressure on the Mg/Fe distribution in olivines. Physics and Chemistry of Minerals, 4, 199–208.

Virgo, D. and Hafner, S. S. (1972) Temperature-dependent Mg, Fe distribution in lunar olivine. Earth and Planetary Science Letters, 14, 305–312.

Wood, B. J. (1974) Crystal field spectrum of Ni^{2+} in olivine. American Mineralogist, 59, 244–248.